

Supporting Information

Bioinspired Holographically-Featured Superhydrophobic and Supersticky Nanostructured Materials

By Sung-Gyu Park[†], Jun Hynk Moon[‡], Seung-Kon Lee[†], JaeWon Shim[†], and Seung-Man Yang^{†,}*

[[†]] Prof. S. -M. Yang, S. -G. Park, Dr. S. -K. Lee, and J.W. Shim
National Creative Research Initiative Center for Integrated Optofluidic Systems;
Department of Chemical and Biomolecular Engineering,
Korea Advanced Institute of Science and Technology
335 Gwahangno, Yuseong-gu, Daejeon, 305-701 (Korea)
Phone: +82-42-350-3962
Fax: +82-42-350-5962
E-mail: smyang@kaist.ac.kr

[[‡]] Prof. J. H. Moon
Department of Chemical & Biomolecular Engineering
Sogang University
1 Shinsu-dong, Mapo-gu, Seoul, 121-742 (Korea)

This supplementary information includes

Supplementary Figures (Figure S1-S9)

Supplementary Table

Supplementary Video Captions

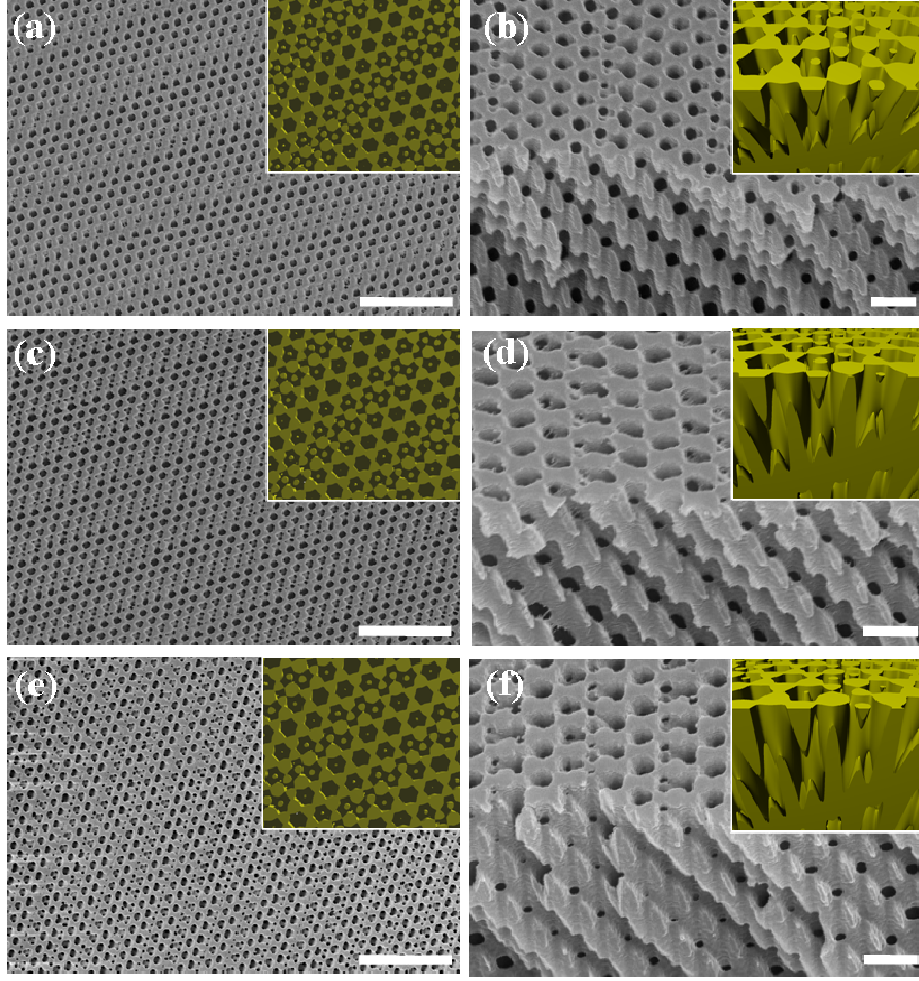


Figure S1. Controlling three-dimensional (3D) nanostructures by tilting the prism to perpendicular incidence of the laser beam. Scanning electron microscope (SEM) images of 3D interference patterns when the prism is tilted an angle of (a) 1.5°, (c) 2.5° and (e) 3.0° with respect to the perpendicularly incident laser beam. The period of the transient layer in (a), (c) and (e) was 3.9 μm , 2.2 μm and 1.8 μm , respectively. The wave vectors of the four beams with tilting angles of 1.5°, 2.5° and 3.0° are $\{\mathbf{k}_0', \mathbf{k}_1', \mathbf{k}_2', \mathbf{k}_3'\} = 2\pi n/\lambda \{[-0.026 \ 0.000 \ -0.999], [-0.305 \ -0.176 \ -0.936], [0.305 \ -0.176 \ -0.936], [0.000 \ 0.352 \ -0.936]\}$, $\{\mathbf{k}_0', \mathbf{k}_1', \mathbf{k}_2', \mathbf{k}_3'\} = 2\pi n/\lambda \{[-0.029 \ 0.000 \ -0.999], [-0.298 \ -0.172 \ -0.939], [0.298 \ -0.172 \ -0.939], [0.000 \ 0.345 \ -0.939]\}$ and $\{\mathbf{k}_0', \mathbf{k}_1', \mathbf{k}_2', \mathbf{k}_3'\} = 2\pi n/\lambda \{[-0.035 \ 0.000 \ -0.999], [-0.295 \ -0.170 \ -0.940], [0.295 \ -0.170 \ -0.940], [0.000 \ 0.341 \ -0.940]\}$, respectively, where n is the refractive index of the fused silica prism ($n=1.48$) and λ is the wavelength of the laser ($\lambda=325 \text{ nm}$). Cross-sectional SEM images at the tilting angles of (b) 1.5°, (d) 2.5° and (f) 3.0°. All insets show the iso-intensity surface of the 3D interference pattern at different tilting angles. By changing the tilting angle θ , the period of the transient layer and the inclination of 3D lattices along the [111]

direction can be controlled. Scale bars in (a), (c) and (e) are 5 μm . Scale bars in (b), (d) and (f) are 1 μm .

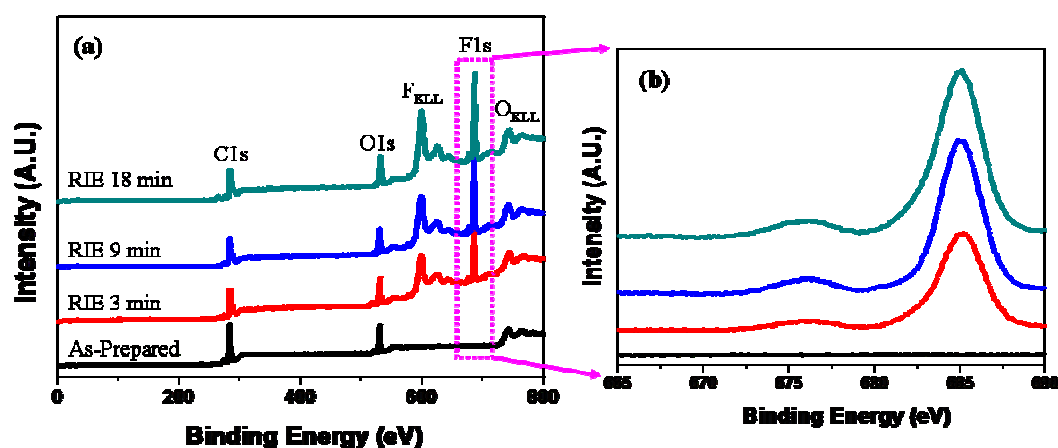


Figure S2. XPS spectra of crosslinked SU-8 thin film for the different RIE times. (a) XPS wide scan spectra. (b) XPS spectra ranging from 665 to 690 eV.

Table S1 Atomic composition of crosslinked SU-8 as determined by XPS analyses according to RIE time.

Treatment	Components		
	C (%)	O (%)	F (%)
As-Prepared	81.7	18.3	0
RIE 3 min	59.8	16.5	23.7
RIE 9 min	51.7	16.1	32.2
RIE 18 min	51.4	16.3	32.3

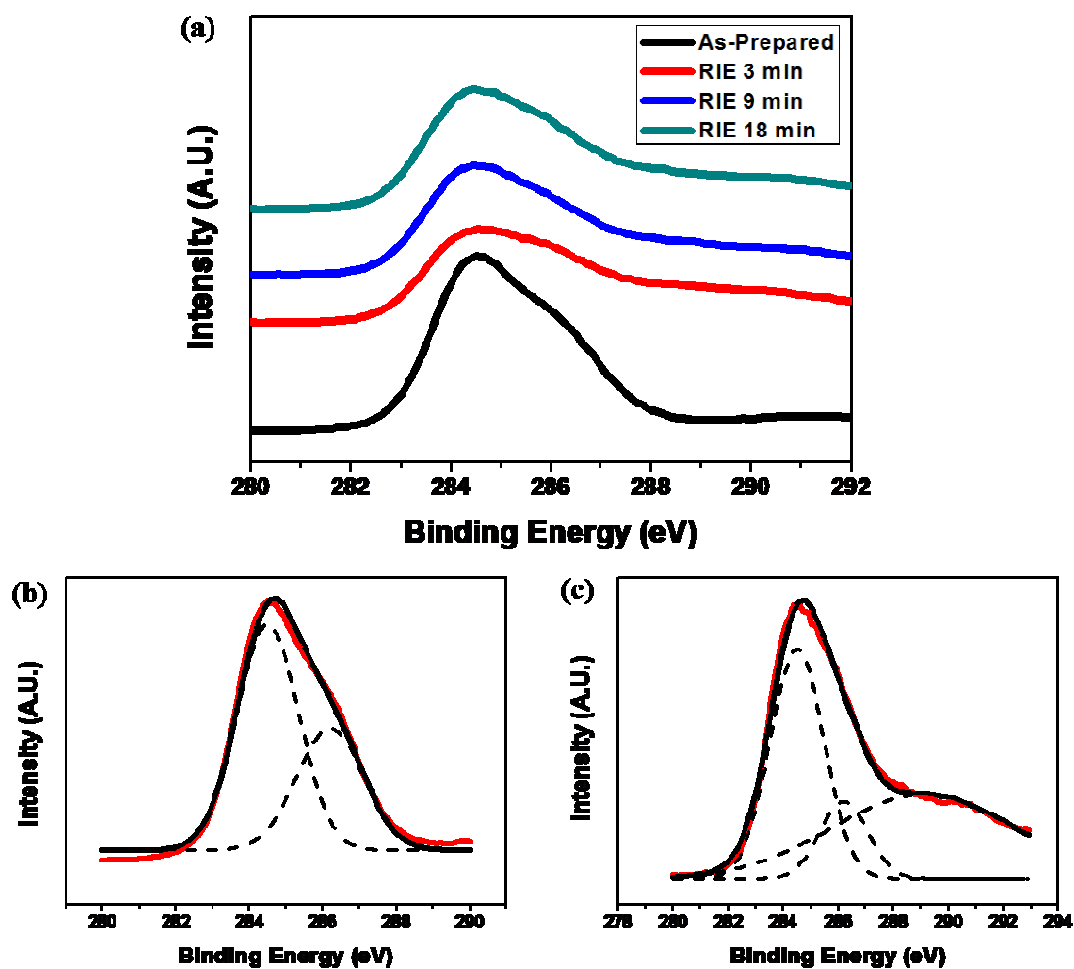


Figure S3. (a) C 1s narrow spectra of the SU-8 surfaces for the different RIE times. High-resolution XPS spectra in the C 1s region for (b) the as-prepared SU-8 film and (c) the modified SU-8 film after 18 min CF_4 RIE. Scale in (b) is not the same as that in (c).

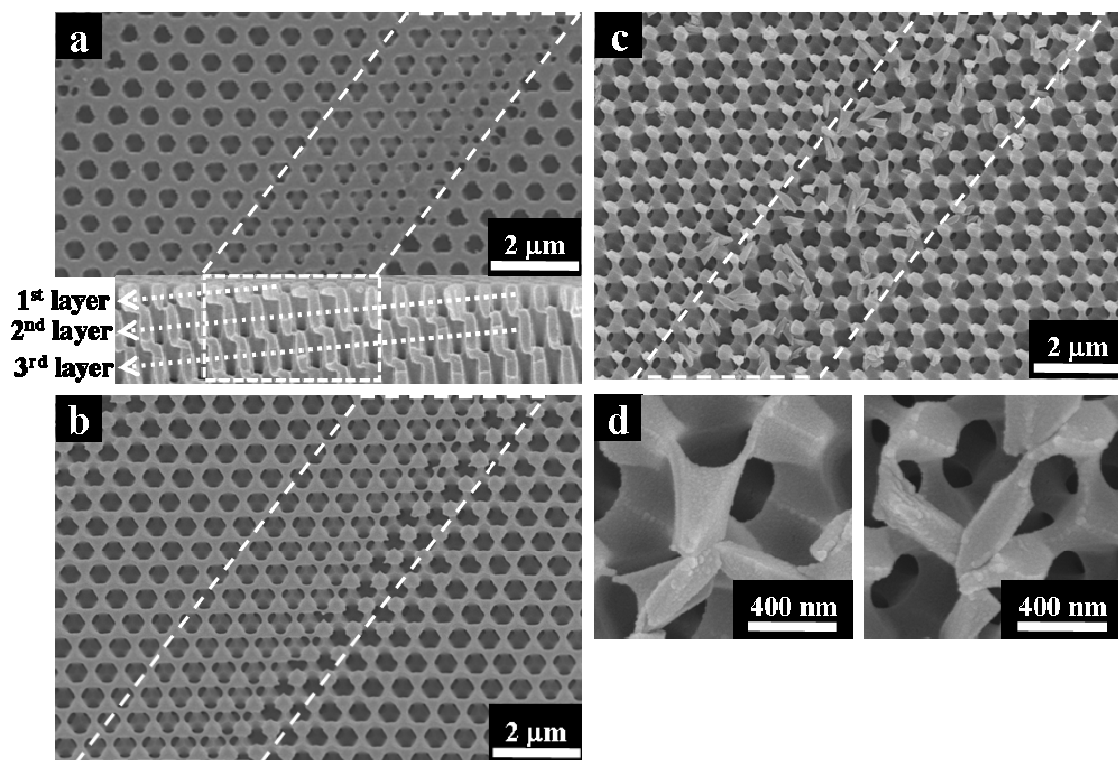


Figure S4. RIE effect on the tilted surface morphology of 3D structures generated by HL. (a) SEM image of the 3D SU-8 interference pattern at a tilting angle of 0.8°. The width of the transient region is about 3 μm. Inset shows a cross-sectional SEM image displaying the atoms in the 1st, 2nd and 3rd layers. (b) SEM images of 3D nanostructures after 6 min of RIE. (c) SEM image of 3D nanostructures after 18 min of RIE. Dotted area represents the transient region in (a), (b) and (c). (d) SEM images of collapsed atoms in the transient region.

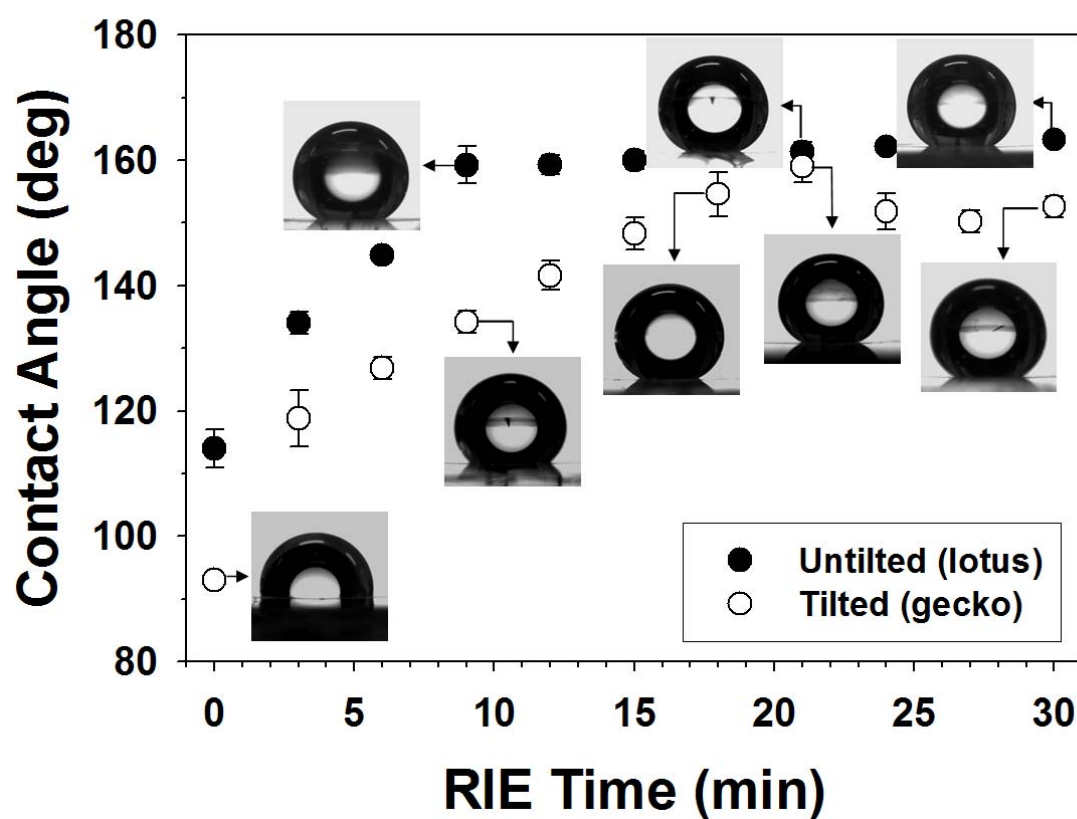


Figure S5. The overall CA measurements according to RIE time. Untilted surface reaches lotus state superhydrophobicity after 9 min of RIE, while the tilted surface exhibits gecko state superhydrophobicity after 18 min of RIE.

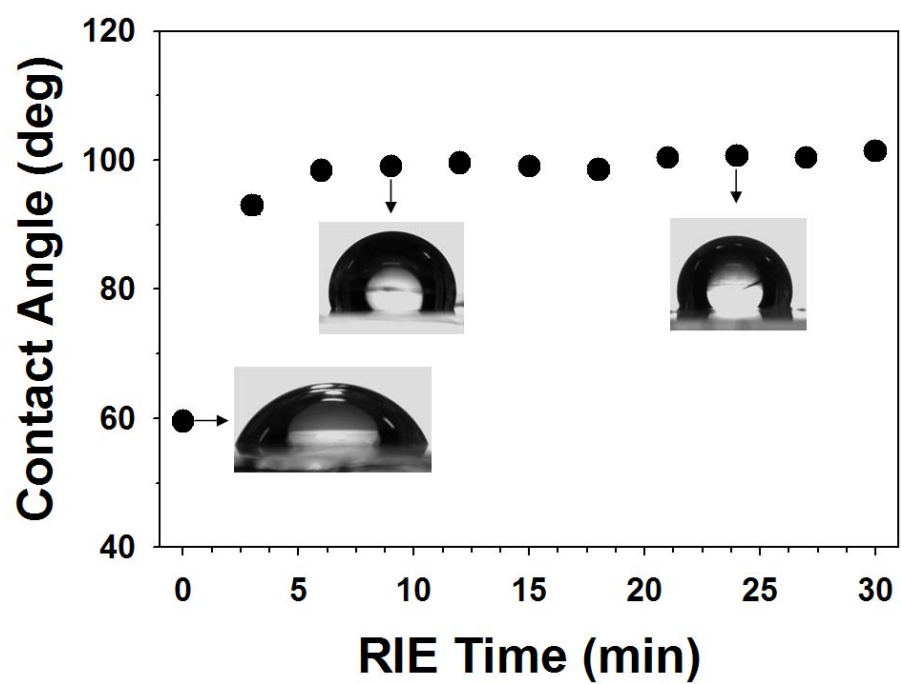


Figure S6. CA measurements of the crosslinked SU-8 smooth surfaces as a function of the RIE time.

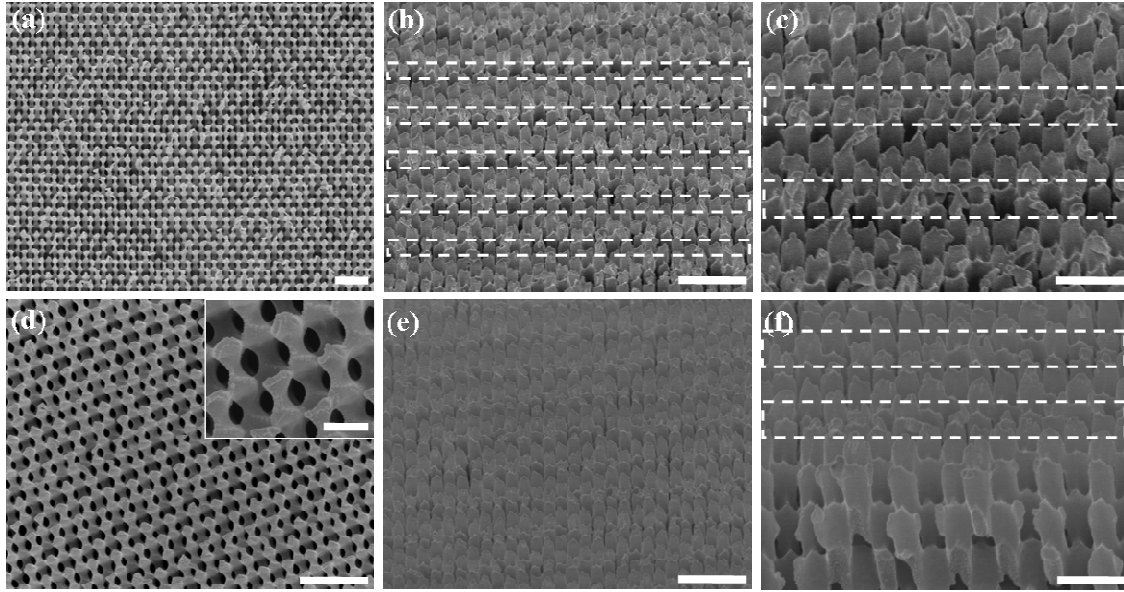


Figure S7. RIE effect on the tilted surface morphology of 3D nanostructures generated by HL. (a) SEM image of 3D nanostructures after 18 min of RIE when the prism is tilted an angle of 2.5° . (b), (c) Magnified tilted SEM images of (a). (d) SEM image of 3D nanostructures after 18 min of RIE when the prism is tilted an angle of 3.0° . Inset shows short blunt tips of unit atoms. Unlike the unetched 3D structures with prism tilting angle of 0.8° , the unetched bridges connecting the atoms are wide, and the unetched atoms are relatively long due to the inclination of 3D lattice along the $[111]$ direction. Due to these surface structures, short blunt tips of unit atoms are created after 18 min of CF_4 RIE. This leads to low CA and full wetting of water droplet. (e), (f) Magnified tilted SEM images of (d). The periods of the transient layer were same with those of as-prepared samples. White dotted area shows transient region. Scale bar in (a), (b), (d) and (e) are $2\ \mu\text{m}$. Scale bars in (c) and (f) are $1\ \mu\text{m}$. Scale bar in inset of (d) is $500\ \text{nm}$.

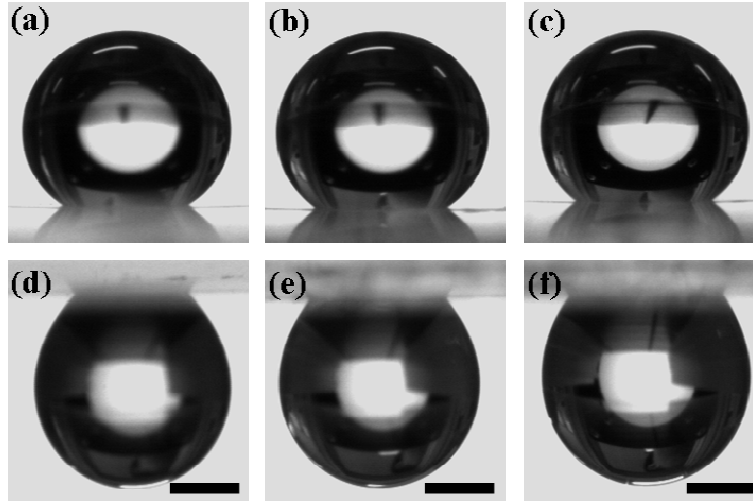


Figure S8. Tilting angle effect on wettability. (a) Hydrophobic wetted surface with a CA of 145° after 18 min of RIE when the prism is tilted an angle of 1.5° . (b) Hydrophobic wetted surface with a CA of 140° after 18 min of RIE when the prism is tilted an angle of 2.5° . (c) Hydrophobic wetted surface with a CA of 136° after 18 min of RIE when the prism is tilted an angle of 3.0° . (d), (e) and (f) Profiles of water droplets of (a), (b) and (C), respectively, when the surface was upside down. All scale bars are 1 mm.

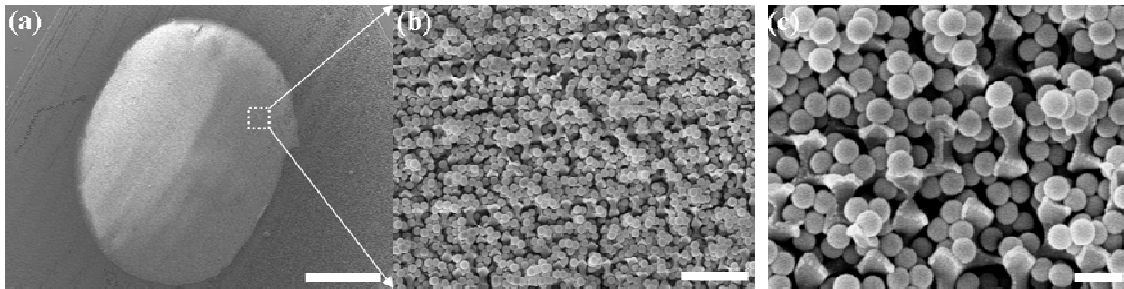


Figure S9. Full wetting. (a) Low magnification SEM image after detaching the dried colloidal crystals. Small anisotropic wetting was observed along the transient layer. (b), (c) Magnified SEM images of (a). Silica particles are fully wetted into the 3D nanostructures due to the surface morphology. Scale bars in (a), (b) and (c) are $500\ \mu\text{m}$, $2\ \mu\text{m}$ and $500\ \text{nm}$, respectively.

Video S1. Placing a 5- μ l water droplet on the lotus state superhydrophobic surface.

This video shows that placing a 5- μ l water droplet on conical-shaped structures with a tip diameter of 40 nm generated by 21 min of RIE is very difficult due to the slippery nature of the surface. All of the samples subjected to 9 min or more of RIE had slippery surfaces. The CA of the surface shown is 161.3°.

Video S2. Sliding Angle (SA) of the lotus state superhydrophobic surface. The SA of the lotus state superhydrophobic surface after 30 min of RIE is about 3°. The SA of a 5- μ l water droplet on the untilted surface subjected to 9 or more minutes of RIE is less than 3°.

Video S3. High adhesion force of the gecko state superhydrophobic surface. This surface after 30 min of RIE holds a 13-mg water droplet when the surface is upside down, and the water droplet does not fall off during vibration.

Video S4. Transferring 5 and 8 mg water droplets from the lotus state to the gecko state superhydrophobic surface with no loss of water. This video shows that 5 and 8 mg water droplets on the lotus state superhydrophobic surface after 30 min of RIE are transferred to gecko state superhydrophobic surface after 30 min of RIE.